Spectral moments in the homogeneous electron gas

M. Vogt,[1] R. Zimmermann,[2] and R. J. Needs[1]
[1]*Theory of Condensed Matter Group, Cavendish Laboratory, Cambridge CB3 0HE, United Kingdom*
[2]*AG Halbleitertheorie, Institut für Physik, Humboldt-Universität zu Berlin, Newtonstrasse 15, 12489 Berlin, Germany*
(Received 10 July 2003; revised manuscript received 17 October 2003; published 30 January 2004)

We present calculations of the lowest three moments of the spectral function of the one-particle Green's function of the unpolarized three-dimensional homogeneous electron gas, which are related to the exact ground-state properties via commutation relations. The moments are, in turn, related to the coefficients in the expansion of the self-energy in inverse powers of the frequency. The zeroth-order term in this expansion can be written in terms of the momentum distribution function, while the first-order term consists of a local term which can be written in terms of the pair correlation function or static structure factor, and a nonlocal term. We use data from diffusion quantum Monte Carlo calculations to evaluate the zeroth-order term and the local part of the first-order term. We have also examined local-field approximations to the self-energy, finding that they do not affect the zeroth-order term in the high-energy expansion, but they substantially alter the first-order term. The nonlocal part of the second-order term has been evaluated using a wave function consisting of a single determinant of plane waves. Our results provide additional benchmarks for self-energy theories of the homogeneous electron gas.

DOI: 10.1103/PhysRevB.69.045113 PACS number(s): 71.10.Ca, 05.30.Fk

I. INTRODUCTION

One of the most important systems for investigating electrons in condensed matter is the homogeneous electron gas (HEG) or jellium model.[1] This widely studied model has yielded many insights into electronic many-body phenomena. However, our knowledge of important dynamical properties of the HEG, such as the one-particle Green's function or equivalently the self-energy, is still far from satisfactory. For example, recent calculations of the quasiparticle energies of the HEG at the density appropriate for sodium predict an occupied bandwidth of about 3.6 eV,[2–4] which is much larger than the values measured in angle-resolved photoemission spectroscopy experiments on sodium of 2.5–2.65 eV.[5,6] At present it is unclear whether this discrepancy is due to an inappropriate interpretation of the experimental data, an inadequacy of present theories of the HEG or shortcomings in the HEG as a model of sodium.

Our goal is to investigate self-energy theories of the HEG and provide benchmarks against which self-energy approximations may be tested. One approach is to calculate static ground-state properties within a given self-energy theory and compare them with the most accurate data available. The most accurate approach for calculating static ground-state properties is currently the diffusion quantum Monte Carlo (QMC) method.[7] Results along these lines have been published, for example, for the total energy.[8–13] In this paper we develop a closely related strategy using the relationship of the moments of the spectral function of the Green's function to the coefficients in the expansion of the self-energy in inverse powers of the frequency (the ''high-energy'' expansion). The corresponding sum rules are valid for the exact self-energy, and were used by von Barth and Holm[8,9] to check the accuracy of their self-consistent *GW* calculation for the HEG. Farid[14] has derived general expressions for the coefficients in the high-energy expansion starting from a real-space description. In our paper these terms are derived in k space for the special case of the HEG.

The zeroth-order term in the expansion of the self-energy is determined by the momentum distribution function and is equivalent to an expression already used by von Barth and Holm.[8] We show how this term changes when we replace the noninteracting Hartree-Fock (HF) momentum distribution by the interacting one, which is obtained from QMC data. The first-order term is the sum of a local and a nonlocal contribution. We show that the expression for the local contribution to the first-order term can be written in terms of the static structure factor. The well-known G_0W_0 approximation to the self-energy includes the zeroth-order term at the noninteracting level and the local contribution to the first-order term within the RPA, but the nonlocal contribution to the first-order term is absent. It is shown that the inclusion of local-field corrections changes the value of the first-order term significantly but preserves its momentum independent form. An approximate calculation of the nonlocal term is presented. The inclusion of nonlocal effects changes the first-order term quantitatively and qualitatively, indicating that these effects are important for calculating the vertex function.

This paper is organized as follows. A short introduction to the jellium model is given in Sec. II. Exact relations for the moments of the spectral function and the coefficients of the high-energy expansion are given, and the corresponding diagrams are given in Sec. III. Approximate self-energy theories used for later comparisons are introduced in Sec. IV. In Sec. V we present our results for the first two coefficients in the self-energy expansion and the first and second moments of the spectral function and show that the higher moments diverge in the HEG. We draw our conclusions in Sec. VI and present an outlook for future investigations. The derivations of the exact expressions for the first and second moments are given in the two appendixes.

II. THE JELLIUM MODEL

The Hamiltonian of the HEG is

$$\hat{H}=\sum_{\mathbf{k},\sigma}\epsilon_0(\mathbf{k})a^+_{\mathbf{k}\sigma}a_{\mathbf{k}\sigma}+\frac{1}{2\Omega}\sum_{\mathbf{q}}v(\mathbf{q})(\hat{\rho}_{\mathbf{q}}\hat{\rho}_{-\mathbf{q}}-\hat{N}), \quad (1)$$

where $\hat{\rho}_{\mathbf{q}}$ is the density operator and $\hat{N}$ is the number operator,

$$\hat{\rho}_{\mathbf{q}}=\sum_{\mathbf{k}\sigma}a^+_{\mathbf{k}\sigma}a_{\mathbf{k}+\mathbf{q}\sigma}, \quad \hat{N}=\sum_{\mathbf{k}\sigma}a^+_{\mathbf{k}\sigma}a_{\mathbf{k}\sigma}, \quad (2)$$

and $a^+_{\mathbf{k}\sigma}(a_{\mathbf{k}\sigma})$ are the fermionic creation (annihilation) operators. The free dispersion $\epsilon_0(\mathbf{k})$ and the Coulomb potential $v(\mathbf{q})$ are given by

$$\epsilon_0(\mathbf{k})=\frac{\hbar\mathbf{k}^2}{2m}, \quad v(\mathbf{q})=\frac{4\pi e^2}{q^2}. \quad (3)$$

It is understood that in the $\mathbf{q}$ summation of Eq. (1) and all following equations, the $\mathbf{q}=0$ term is omitted, which follows from the cancellation of this term with that from the uniform positive background. The uniform charge density is $n_0=N_e/\Omega$, where N_e electrons occupy a volume Ω. The properties of the HEG are usually written in terms of the dimensionless parameter r_s, which is related to the electron density by $1/n_0=4\pi r_s^3 a_0^3/3$, where a_0 is the Bohr radius. Since the density is given in terms of the Fermi momentum k_f as $n_0=k_f^3/3\pi^2$, we have the relation

$$k_f=\frac{1}{\alpha r_s a_0}, \quad \alpha=\left(\frac{4}{9\pi}\right)^{1/3}\approx 0.521\,06. \quad (4)$$

All quantities in this paper are given in units of E_f and k_f. To convert quantities from units of E_f to atomic units one divides by $2(\alpha r_s)^2$.

III. EXACT RELATIONS FOR THE SPECTRAL MOMENTS

A. Spectral functions

In a translationally invariant system such as the HEG the Green's function $G_\sigma(\mathbf{k},\omega)$ and self-energy $\Sigma_\sigma(\mathbf{k},\omega)$ are related by

$$G_\sigma(\mathbf{k},\omega)=\frac{1}{\omega-\epsilon_0(\mathbf{k})-\Sigma_\sigma(\mathbf{k},\omega)}. \quad (5)$$

In the spectral representation the Green's function is written as

$$G_\sigma(\mathbf{k},\omega)=\int_{-\infty}^{\infty}d\omega'\frac{A_\sigma(\mathbf{k},\omega')}{\omega-\omega'+i\delta\,\mathrm{sgn}(\omega'-\mu)}, \quad (6)$$

where $A_\sigma(\mathbf{k},\omega)$ is the spectral function and μ is the chemical potential. The spectral function is therefore related to the imaginary part of the Green's function by

$$A_\sigma(\mathbf{k},\omega)=\frac{1}{\pi}|\mathrm{Im}G_\sigma(\mathbf{k},\omega)|, \quad (7)$$

or explicitly, using Eq. (5),

$$A_\sigma(\mathbf{k},\omega)=\frac{1}{\pi}\frac{|\mathrm{Im}\Sigma_\sigma(\mathbf{k},\omega)|}{[\omega-\epsilon_0(\mathbf{k})-\mathrm{Re}\Sigma_\sigma(\mathbf{k},\omega)]^2+[\mathrm{Im}\Sigma_\sigma(\mathbf{k},\omega)]^2}. \quad (8)$$

The frequency moments of the spectral function are defined as

$$M^{(n)}_{\mathbf{k}\sigma}=\int_{-\infty}^{\infty}d\omega\,\omega^n A_\sigma(\mathbf{k},\omega). \quad (9)$$

The self-energy can also be written in terms of a spectral function,

$$\Sigma_\sigma(\mathbf{k},\omega)=\Sigma_{x,\sigma}(\mathbf{k})+\int d\omega'\frac{C_\sigma(\mathbf{k},\omega')}{\omega-\omega'+i\delta\,\mathrm{sgn}(\omega'-\mu)}, \quad (10)$$

where $\Sigma_{x,\sigma}(\mathbf{k})$ is the frequency-independent exchange term whose structure will be discussed below.

B. General relation between the spectral moments and the high-energy expansion of the self-energy

Expanding the denominator in Eq. (6) one obtains

$$G_\sigma(\mathbf{k},\omega)=\sum_{n=1}^{n_1+1}\frac{M^{(n-1)}_{\mathbf{k}\sigma}}{\omega^n}+f_1(\mathbf{k},\omega), \quad (11)$$

where $f_1(\mathbf{k},\omega)$ is a quantity decaying faster than $\omega^{-(n_1+1)}$, and n_1 is the order up to which the moments are finite. (In Sec. V D we show that $n_1=2$ for the HEG.)

A similar expression is expected to hold for the self-energy

$$\Sigma_\sigma(\mathbf{k},\omega)=\sum_{p=0}^{n_1-1}\frac{\Sigma^{(p)}_{\mathbf{k}\sigma}}{\omega^p}+f_2(\mathbf{k},\omega), \quad (12)$$

where $f_2(\mathbf{k},\omega)$ is a function decaying faster than $\omega^{-(n_1-1)}$. By inserting Eqs. (11) and (12) into Eq. (5), expanding the right-hand side of Eq. (5), and equating the coefficients of powers of $1/\omega$ we obtain

$$M^{(0)}_{\mathbf{k}\sigma}=1, \quad \Sigma^{(0)}_{\mathbf{k}\sigma}=M^{(1)}_{\mathbf{k}\sigma}-\epsilon_0(\mathbf{k}), \quad (13)$$

and

$$\Sigma^{(1)}_{\mathbf{k}\sigma}=M^{(2)}_{\mathbf{k}\sigma}-(M^{(1)}_{\mathbf{k}\sigma})^2. \quad (14)$$

It is a general property of these relations that the pth coefficient $\Sigma^{(p)}_{\mathbf{k}\sigma}$ is determined by the spectral moments up to order $p+1$.

C. Derivation of the first and the second moments

The nth moment of the spectral function is given by the nth derivative with respect to time t of the time-dependent spectral function,[15]

$$A_\sigma(\mathbf{k},t)=\langle[a_{\mathbf{k}\sigma}(t),a^+_{\mathbf{k}\sigma}(0)]_+\rangle, \tag{15}$$

evaluated at $t=0$. By calculating these derivative using the Heisenberg equation of motion we get an n-fold nested commutator with the Hamilton operator $\hat{H}$,

$$M^{(n)}_{\mathrm{k}\sigma}=\langle[\underbrace{[\ldots[a_{\mathrm{k}\sigma},\hat{H}]_-\ldots,\hat{H}]_-}_{n\text{-}times},a^+_{\mathrm{k}\sigma}]_+\rangle, \tag{16}$$

where $\langle\cdots\rangle$ denotes the ground-state expectation value of the system.

The zeroth moment is

$$M^{(0)}_{\mathbf{k}\sigma}=\langle[a_{\mathbf{k}\sigma},a^+_{\mathbf{k}\sigma}]_+\rangle=1, \tag{17}$$

which gives the normalization of the spectral function. In Appendix A we show that the first moment of the spectral function of the HEG is given by

$$M^{(1)}_{\mathbf{k}\sigma}=\epsilon_0(\mathbf{k})+\Sigma_{x,\sigma}(\mathbf{k}), \tag{18}$$

where $\Sigma_{x,\sigma}(\mathbf{k})$ is the exchange self-energy

$$\Sigma_{x,\sigma}(\mathbf{k})=-\frac{1}{\Omega}\sum_{\mathbf{q}} v(\mathbf{k}-\mathbf{q})n_{\mathbf{q}\sigma}, \tag{19}$$

and $n_{\mathbf{k}\sigma}$ is the expectation value of the number operator

$$n_{\mathbf{k}\sigma}=\langle a^+_{\mathbf{k}\sigma}a_{\mathbf{k}\sigma},\rangle, \tag{20}$$

i.e., the exact momentum distribution function. From Eqs. (13) and (18) one obtains

$$\Sigma^{(0)}_{\mathbf{k}\sigma}=\Sigma_{x,\sigma}(\mathbf{k}). \tag{21}$$

Equation (18) has been derived, for example, by von Barth and Holm[8] directly from the spectral representation of the Green's function and the self-energy.

For the second moment we find, see Appendix B,

$$\begin{aligned}M^{(2)}_{\mathbf{k}\sigma}=&\epsilon_0^2(\mathbf{k})+2\epsilon_0(\mathbf{k})\Sigma^{(0)}_{\mathbf{k}\sigma}+\frac{1}{\Omega^2}\sum_{\mathbf{q}} v^2(\mathbf{q})\\&\times\langle\hat{\rho}_{\mathbf{q}}\hat{\rho}_{-\mathbf{q}}\rangle-\frac{1}{\Omega^2}\sum_{\mathbf{q}\mathbf{q}'} v(\mathbf{q})v(\mathbf{q}')n_{\mathbf{k}-\mathbf{q}-\mathbf{q}'\sigma}\\&-\frac{2}{\Omega^2}\sum_{\mathbf{q}\mathbf{q}'} v(\mathbf{q})v(\mathbf{q}')\langle a^+_{\mathbf{k}-\mathbf{q}'\sigma}\hat{\rho}_{\mathbf{q}}a_{\mathbf{k}-\mathbf{q}-\mathbf{q}'\sigma}\rangle.\end{aligned} \tag{22}$$

Let us discuss the structure of the second moment in detail. First we note the existence of a momentum- and spin-independent term in the second line which can be rewritten in terms of the static structure factor,[1]

$$S(\mathbf{q})=-N_e\delta_{\mathbf{q},0}+\frac{1}{N_e}\langle\hat{\rho}_{\mathbf{q}}\hat{\rho}_{-\mathbf{q}}\rangle. \tag{23}$$

Since $\mathbf{q}=0$ has to be omitted in the $\mathbf{q}$ summation, we obtain

$$\frac{1}{\Omega^2}\sum_{\mathbf{q}} v^2(\mathbf{q})\langle\hat{\rho}_{\mathbf{q}}\hat{\rho}_{-\mathbf{q}}\rangle=\frac{n_0}{\Omega}\sum_{\mathbf{q}} v^2(\mathbf{q})S(\mathbf{q}). \tag{24}$$

It follows from Eqs. (14), (18), and (22) that $\Sigma^{(1)}_{\mathbf{k}\sigma}$ consists of a local, spin-independent contribution and a nonlocal, spin-dependent contribution,

$$\Sigma^{(1)}_{\mathbf{k}\sigma}=\Sigma^{(1)}_{\mathrm{loc}}+\Sigma^{(1)}_{\mathrm{nl},\mathbf{k}\sigma} \tag{25}$$

with

$$\Sigma^{(1)}_{\mathrm{loc}}=\frac{n_0}{\Omega}\sum_{\mathbf{q}} v^2(\mathbf{q})S(\mathbf{q}), \tag{26}$$

and

$$\begin{aligned}\Sigma^{(1)}_{\mathrm{nl},\mathbf{k}\sigma}=&-\frac{1}{\Omega^2}\sum_{\mathbf{q}\mathbf{q}'} v(\mathbf{q})v(\mathbf{q}')n_{\mathbf{k}-\mathbf{q}-\mathbf{q}'\sigma}-\frac{2}{\Omega^2}\sum_{\mathbf{q}\mathbf{q}'} v(\mathbf{q})v(\mathbf{q}')\\&\times\langle a^+_{\mathbf{k}-\mathbf{q}'\sigma}\hat{\rho}_{\mathbf{q}}a_{\mathbf{k}-\mathbf{q}-\mathbf{q}'\sigma}\rangle-(\Sigma^{(0)}_{\mathbf{k}\sigma})^2.\end{aligned} \tag{27}$$

One can show that the second term in Eq. (27) is real since the ground-state wave function of the HEG can always be chosen to be real.

Farid[14] has calculated the first three terms in the high-energy expansion of the self-energy for systems of spin-half fermions in d-dimensional $\mathbf{r}$ space, interacting through an arbitrary two-body potential $v(\mathbf{r}-\mathbf{r}')$. For the first-order term he found a local spin independent and a nonlocal spin-dependent contribution as well. After Fourier transforming, our expressions (25) and (27) for the HEG are equivalent to special cases of Farid's.

IV. APPROXIMATE THEORIES OF THE SELF-ENERGY OF THE HEG

In this section we introduce approximations to the self-energy which have been widely used in earlier work. We will discuss some of these approximations later within the framework of the previously derived exact relations. The self-energy can be written as

$$\begin{aligned}\Sigma(\mathbf{k},\omega)=&\frac{i}{(2\pi)^4}\int d^3q\,d\omega' G(\mathbf{k}+\mathbf{q},\omega+\omega')\\&\times W(\mathbf{q},\omega')\Gamma(\mathbf{k},\omega,\mathbf{k}+\mathbf{q},\omega+\omega'),\end{aligned} \tag{28}$$

where Γ is the vertex function. The dynamically screened interaction potential W is defined as

$$W(\mathbf{q},\omega)=\frac{v(\mathbf{q})}{\epsilon(\mathbf{q},\omega)}=\frac{v(\mathbf{q})}{1-v(\mathbf{q})P(\mathbf{q},\omega)}, \tag{29}$$

where $\epsilon(\mathbf{q},\omega)$ is the dielectric function and P is the irreducible polarization propagator

$$P(\mathbf{q},\omega) = -\frac{2i}{(2\pi)^4}\int d^3k d\omega' G(\mathbf{q}+\mathbf{k},\omega+\omega') \times G(\mathbf{k},\omega')\Gamma(\mathbf{k},\omega',\mathbf{q}+\mathbf{k},\omega+\omega'). \quad (30)$$

Together with Eq. (5) and the expression for the vertex function these equations form a self-consistent set of equations known as Hedin's equations.[16,17] The fundamental problem lies in an appropriate choice of the vertex function.

Self-consistent calculations of the self-energy using a sophisticated ansatz for the full vertex function have been presented.[2–4] The resulting occupied bandwidth is broader than the free-electron result and much broader than the experimental data. According to Yasuhara *et al.*[2] these results may be made consistent with the experimental observations by considering final state effects, although this idea has been sharply criticized.[18]

A first approximation is to set the vertex function equal to unity. Because of the resulting structure of the self-energy this scheme is called the *GW* approximation, and was first proposed by Hedin.[16] Barth and Holm[9] performed self-consistent *GW* calculations for the HEG and found an increase in the valence bandwidth compared with the free-electron result as well as a broad and featureless satellite structure. However, both results contradict experiment. A significant improvement for the satellite structure has been obtained using a self-consistent cumulant expansion.[19]

Another approximation is to replace the interacting Green's function by the noninteracting Green's function G_0, but to retain the vertex functions in Eqs. (28) and (30) in a simplified form, as $\Gamma(\mathbf{q},\omega)$. Such a scheme has been used, for example, to study quasiparticle properties.[1,10] In this approximation the self-energy is written as

$$\Sigma(\mathbf{k},\omega) = \frac{i}{(2\pi)^4}\int d^3q d\omega' G_0(\mathbf{k}+\mathbf{q},\omega + \omega')W(\mathbf{q},\omega')\Gamma(\mathbf{q},\omega'), \quad (31)$$

and

$$W(\mathbf{q},\omega) = \frac{v(\mathbf{q})}{\epsilon(\mathbf{q},\omega)} = \frac{v(\mathbf{q})}{1-v(\mathbf{q})\Gamma(\mathbf{q},\omega)P_0(\mathbf{q},\omega)}, \quad (32)$$

where the independent-electron polarizability P_0 is given by

$$P_0(\mathbf{q},\omega) = -\frac{2i}{(2\pi)^4}\int d^3k d\omega' G_0(\mathbf{k}+\mathbf{q},\omega+\omega')G_0(\mathbf{k},\omega'). \quad (33)$$

Assuming the simplified form of the vertex function $\Gamma(\mathbf{q},\omega)$ a summation of ladder diagrams leads to

$$\Gamma(\mathbf{q},\omega) = \frac{1}{1+v(\mathbf{q})f(\mathbf{q})P_0(\mathbf{q},\omega)}, \quad (34)$$

where $f(\mathbf{q})$ is the local-field factor. From Eqs. (32) and (34) we obtain for the dielectric function

$$\epsilon(\mathbf{q},\omega) = 1 - \frac{v(\mathbf{q})P_0(\mathbf{q},\omega)}{1+v(\mathbf{q})f(\mathbf{q})P_0(\mathbf{q},\omega)}. \quad (35)$$

We call this scheme the local-field approximation. Results for the HEG give a narrowing of the occupied bandwidth.[20]

Various forms of the local-field factor have been suggested over the years. Hubbard (H) derived the form $f_{\mathrm{H}}(q) = q^2/2(q^2+1)$.[21] An improved theory of the local-field factor was suggested by Singwi, Tosi, Land, and Sjölander (STLS).[22] Vashishta and Singwi (VS) modified the STLS theory so that it almost exactly fulfills the compressibility sum rules.[23] The VS expression can be adequately fitted by the form $f_{\mathrm{VS}}(q) = A[1-\exp(-Bq^2)]$, where A and B are fitting parameters.[23]

In some studies in the 1980s[24,25] quasiparticle properties were calculated by including the vertex correction in the expression for the screened interaction of Eq. (32) but not in the self-energy integral. This approximation leads to a valence bandwidth very close to the experimental data. It is, however, an inconsistent approach.

In their original work on the *GW* approximation Hedin[16] and later Lundqvist[26] solved Eqs. (31) and (32) for $f(\mathbf{q}) = 0$, i.e., $\Gamma(\mathbf{q},\omega) = 1$. This is equivalent to using the well-known Lindhard or random phase approximation (RPA) dielectric function,

$$\epsilon_0(\mathbf{q},\omega) = 1 - v(\mathbf{q})P_0(\mathbf{q},\omega) \quad (36)$$

in the expression for the screened interaction W_0. In this paper we refer to this scheme as the G_0W_0 approximation. Within this approximation the valence bandwidths are close to the values calculated within the local-field approximation.[20]

V. RESULTS AND DISCUSSION

We are specifically interested in the properties of the HEG at metallic densities ($1 < r_s < 5$). Various QMC calculations show that in this region the HEG is unpolarized,[27,28] and we therefore limit ourselves to this case.

A. The zeroth-order term Σ_0

The zeroth-order term corresponds to the well-known diagram for the exchange self-energy [Fig. 1(b)]. If the noninteracting Green's function is used, the diagram represents the HF approximation [Fig. 1(a)].

After inserting Eq. (21) into Eq. (19) and performing the angular integration one obtains for the zeroth-order term

$$\Sigma_k^{(0)} = -\frac{2\alpha r_s}{\pi k}\int_0^\infty dq q n_q \ln\left|\frac{k+q}{k-q}\right|, \quad (37)$$

where we made use of the fact that $n_{\mathbf{q}}$ is isotropic. By inserting the noninteracting momentum distribution of the HEG,

$$n_k^{(0)} = \begin{cases} 1, & k<1 \\ 0, & k>1, \end{cases} \quad (38)$$

into Eq. (37) we obtain the well-known HF result

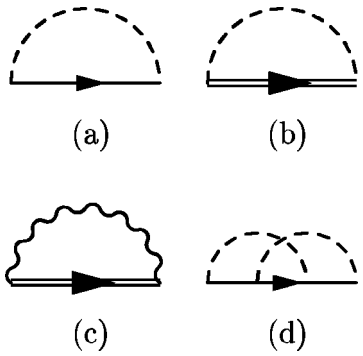

FIG. 1. Self-energy diagrams corresponding to the terms used in this paper. The lines represent the noninteracting Green's function (single solid line), the interacting Green's function (double solid line), the bare Coulomb interaction (dashed line), and the screened interaction (wiggly line). The diagrams represent (a) the exchange self-energy in HF theory, (b) the exact exchange self-energy, (c) the GW self-energy, and (d) the first vertex correction beyond GW in the single-Slater-determinant approximation (SSDA).

$$\Sigma_k^{(\mathrm{HF})} = -\frac{\alpha r_s}{\pi}\left[2+\left(\frac{1}{k}-k\right)\ln\left|\frac{k+1}{k-1}\right|\right]. \tag{39}$$

Note that whenever the noninteracting Green's function is used in obtaining the self-energy, we find $\Sigma_k^{(0)} = \Sigma_k^{(\mathrm{HF})}$.

We have performed calculations of $\Sigma_k^{(0)}$ using different momentum distributions beyond HF. First, we determined n_k from the equation

$$n_k = \int_{-\infty}^{\mu} d\omega A(k,\omega), \tag{40}$$

where $A(k,\omega)$ is the spectral function calculated using the G_0W_0 self-energy in Eq. (8).

Highly accurate momentum distributions have been determined from diffusion QMC calculations. Ortiz and Ballone (OB) (Ref. 29) performed such calculations for a range of values of r_s, and fitted their momentum densities to polynomials, with different forms for q above and below one. A different fitting to the same QMC data was suggested by Senatore, Moroni, and Ceperley (SMC).[30] In a recent paper Gori-Giorgi and Ziesche (GZ) proposed another fitting formula which obeys some other constraints.[31,33] In Fig. 2 we plot the HF, G_0W_0, OB-QMC, and GZ-QMC formulas for $r_s=5$, where the finite jump Z_{k_f} at $k/k_f=1$ is the weight of the quasiparticle at the Fermi edge. The SMC-QMC curve lies very close to the OB-QMC data. One of the distinctive features of the GZ fitting is the infinite that the momentum distribution function approaches the Fermi edge with an infinite slope. This feature resembles the shape of the G_0W_0 momentum distribution. The QMC data are only calculated at k vectors commensurate with the simulation cell used and it is not clear whether QMC calculations closer to the Fermi edge would show such a feature.

The question arises of whether the uncertainties in the correct momentum distribution have a significant impact on our values for $\Sigma_k^{(0)}$. Figure 3 shows $\Sigma_k^{(0)}$ at $r_s=5$, calculated from Eq. (37) using the HF, G_0W_0, OB-QMC, and GZ-QMC momentum distributions. The inclusion of correlation increases $\Sigma_k^{(0)}$ at small k and reduces the dispersion of $\Sigma_k^{(0)}$. The G_0W_0 result is already very close to the QMC data, presenting a significant improvement over the HF curve. The differences between the various QMC fits at small k are almost as large as between the GZ-QMC and G_0W_0 values. This shows that an accurate determination of the shape of the momentum distribution is needed to exclude any ambiguity for this benchmark. However, because the differences between the results obtained with the different QMC fits are small we believe that our values for the first moment are already highly accurate. In Table I we give some numerical values for $\Sigma_k^{(0)}$ obtained at three values of k using the HF, G_0W_0, OB-QMC, SMC-QMC, and GZ-QMC momentum distributions.

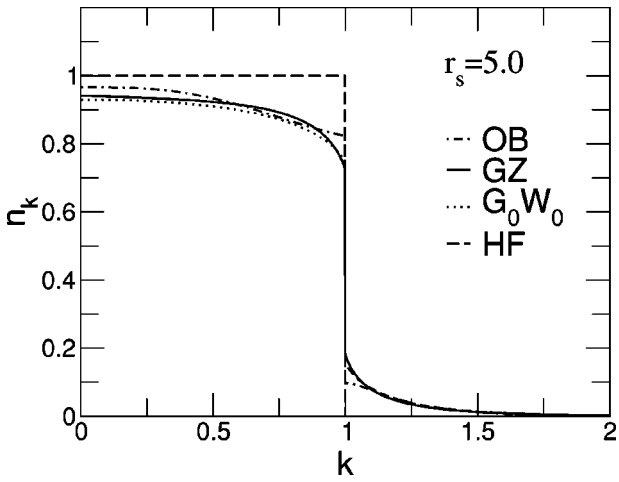

FIG. 2. The momentum distribution function of the HEG at $r_s=5$ within HF and G_0W_0 theory, and from the QMC fitting formulas of Ortiz and Ballone[29] (OB) and Gori-Giorgi and Ziesche[31] (GZ).

B. The local part of the first-order term $\Sigma_{\mathrm{loc}}^{(1)}$

In the high-energy expansion of the self-energy, the first term is the (ω-independent) exchange term, represented by

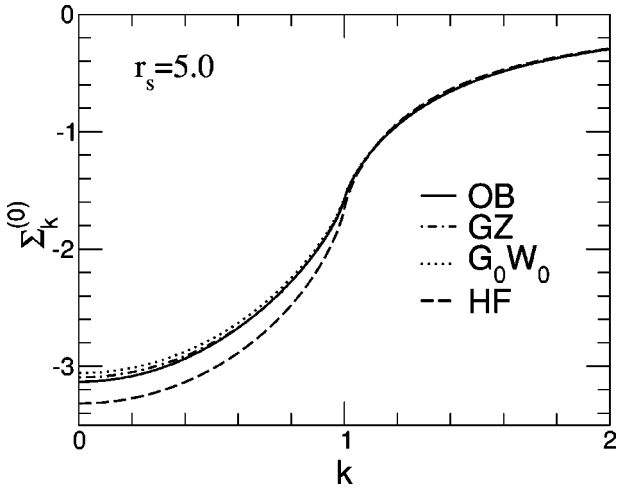

FIG. 3. $\Sigma_k^{(0)}$ for $r_s=5$ calculated from Eq. (37) using the OB-QMC, GZ-QMC, G_0W_0, and HF momentum distributions.

TABLE I. The zeroth-order term $\Sigma_k^{(0)}$ for $r_s=5$ calculated using the HF, G_0W_0, OB, SMC, and GZ-QMC momentum distributions and Eqs. (37) and (18).

k	HF	G_0W_0	OB	SMC	GZ
0.0	−3.317	−3.057	−3.131	−3.114	−3.095
0.6	−2.885	−2.631	−2.673	−2.656	−2.669
1.0	−1.686	−1.573	−1.578	−1.561	−1.573
1.4	−0.640	−0.654	−0.659	−0.662	−0.658

diagram (b) in Fig. 1. The next term goes as $1/\omega$ and contains the difference of diagrams (c)–(b). Since the Green's function $G(k,\omega)\rightarrow 1/\omega$ in the high-energy limit, it does not appear in the final expression for the local term.

The relation to the local term $\Sigma_{\rm loc}^{(1)}$ can be seen by writing the structure factor in terms of the dielectric function $\epsilon(\mathbf{q},\omega)$,[1]

$$S(q)=-\frac{3q^2}{8\alpha r_s}\int_0^\infty d\omega \mathrm{Im}\frac{1}{\epsilon(q,\omega)}. \tag{41}$$

Inserting Eq. (41) into Eq. (26) gives exactly the high-energy limit of Eq. (31) if the vertex function is set to unity, i.e., the GW approximation. Consequently, the G_0W_0 approximation corresponds to using the noninteracting Green's function and the RPA screened potential in the diagram of Fig. 1(c).

The local part of the first-order term is evaluated from Eq. (26). Since $S(\mathbf{q})$ is isotropic we obtain

$$\Sigma_{\rm loc}^{(1)}=\frac{32}{3\pi^2}(\alpha r_s)^2\int_0^\infty \frac{dq}{q^2}S(q). \tag{42}$$

Equations (42) and (41) are equivalent to the expression for the second moment $M_{\mathbf{k}}^{(2)}$ in terms of the spectral function of the self-energy and the screened interaction given by Eq. (17) of the paper by von Barth and Holm.[8]

Diffusion QMC calculations give the pair correlation function $g(r)$ directly.[32] From these data one can calculate highly accurate static structure factors using the relation

$$S(\mathbf{q})-1=n_0\int d^3r e^{i\mathbf{qr}}[g(\mathbf{r})-1]. \tag{43}$$

Equations (42) and (41) therefore enable us to calculate the local term and the second moment within the self-energy approximations introduced in Sec. IV by using the corresponding dielectric function. In addition we study the local term in the HF approximation, where the structure factor is given by

$$S(q)=\begin{cases}\frac{3}{4}q-\frac{1}{16}q^3, & q<2\\ 1, & q>2.\end{cases} \tag{44}$$

Structure factors within the RPA using the dielectric function of Eq. (36) and the VS approximation [$f(\mathbf{q})=f_{\rm VS}(q)$ in Eq. (35)] were calculated from Eq. (41). Ortiz, Harris, and Ballone[28] have performed diffusion QMC calculations of the static structure factor of the HEG, and a fitting formula using this data has been developed by Gori-Giorgi, Sacchetti, and Bachelet (GSB).[32,33] Results for $r_s=5$ and QMC-GSB data for $r_s=1$ are shown in Fig. 4, where we have also included the HF structure factor of Eq. (44). The HF structure factor is linear at small q while the more advanced approximations which include correlation effects are quadratic at small q. The linear dependence in HF theory leads to a divergence of the integral in Eq. (42).[34]

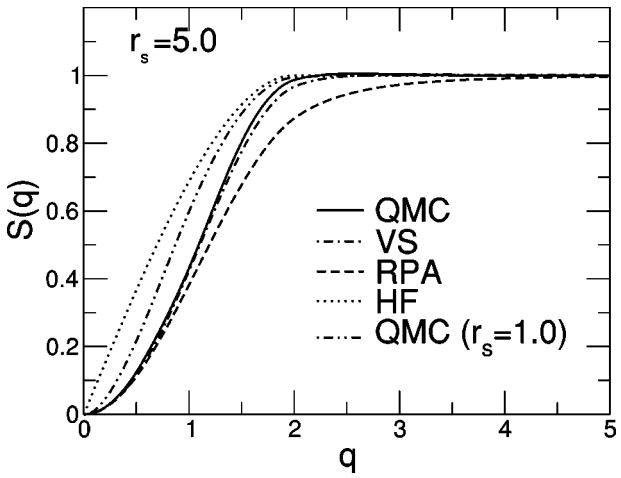

FIG. 4. The structure factor $S(q)$ as a function of q at $r_s=5$. Data from the GSB fitting formula to the QMC data, the HF approximation, and from the RPA and VS dielectric functions are shown. Data for the QMC-GSB structure factor at $r_s=1$ are also presented.

All approximations which go beyond HF theory give finite values of $\Sigma_{\rm loc}^{(1)}$, since the structure factor is proportional to q^2. We calculated $\Sigma_1^{\rm loc}$ from Eq. (42) using the GSB-QMC formula and the RPA and VS local-field approximations for the structure factor (Fig. 5). The main contribution to the integral in Eq. (42) is from the small q region. Figure 4 shows that at small q the values of the structure factors

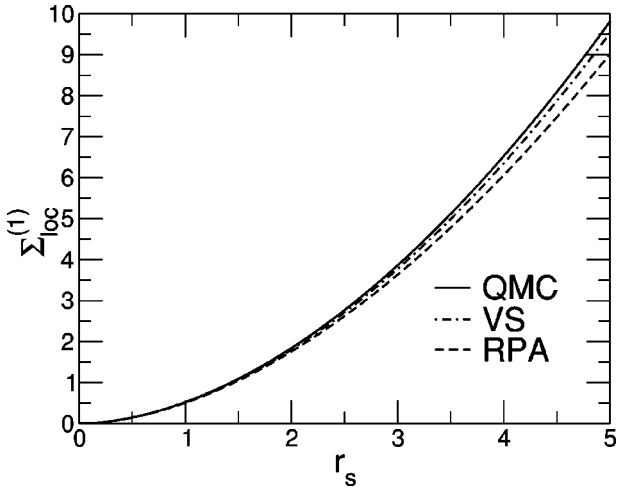

FIG. 5. The local term $\Sigma_{\rm loc}^{(1)}$ as a function of the density parameter r_s calculated using different approximations for the structure factor and the GSB-QMC structure factor in Eq. (42).

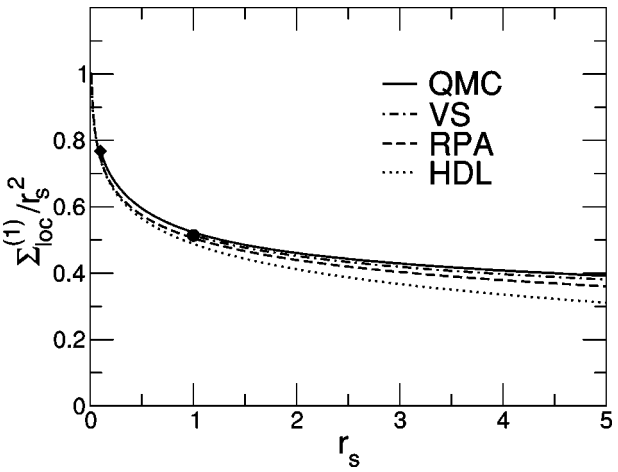

FIG. 6. The ratio $\Sigma^{(1)}_{\rm loc}/r_s^2$ as a function of the density parameter r_s calculated using different approximations for the structure factor and the GSB-QMC structure factor in Eq. (42). In addition we plot this ratio for the high-density limit (HDL) of the RPA Eq. (45). The symbols indicate the lower limit of the range where the fitting formulas for the structure factor in QMC (diamond) and VS (circle) are valid.

which include correlation effects lie almost on top of each other. It is for this reason that the various approximations to $\Sigma^{(1)}_{\rm loc}$ in Fig. 5 are rather similar. The RPA result deviates from the QMC result more than the local-field ones. This reflects the well-known fact that correlation effects are important in the description of the electron gas at metallic densities. The inclusion of local-field effects within $S(q)$ gives results surprisingly close to the QMC data even at quite low densities, with the VS result being closest.

In the high-density limit $S(q)$ approaches the HF result, although the quadratic behavior for $q\rightarrow 0$ is preserved (see the QMC-GSB curve for $r_s=1$ in Fig. 4). This results in a contribution proportional to $r_s^2 \ln r_s$ to $\Sigma^{(1)}_{\rm loc}$ in the high-density limit. In Fig. 6 we plot $\Sigma^{(1)}_{\rm loc}/r_s^2$ as a function of r_s. The RPA data clearly shows the logarithmic divergence at $r_s\rightarrow 0$. It is possible to calculate this leading order term analytically within the RPA, using the strategy of Gell-Mann and Brückner as presented in the review paper by Hedin and Lundqvist,[17] and we obtain

$$\Sigma^{(1)}_{\rm loc}\sim \frac{8}{\pi}(\alpha r_s)^2\left(-\frac{1}{2\pi}\ln r_s + b\right). \tag{45}$$

By fitting the numerical values for small r_s we obtain $b\approx 0.706$. The dotted curve in Fig. 6 corresponds to Eq. (45) with $b=0.706$.

The QMC and VS data follow similar curves to the RPA, but for these cases no data is available at very low r_s. However, the data in Fig. 6 strongly suggests that the logarithmic divergence in the slope is not an artifact of the RPA.

C. The nonlocal part of the first-order term $\Sigma^{(1)}_{\rm nl,k}$

The nonlocal term of Eq. (27) is complicated due to the four-operator expectation value in the second term. The exact calculation of this term within QMC is the subject of ongoing work and will be presented in a forthcoming paper. In the present paper we will analyze the nonlocal term within the single-Slater-determinant approximation (SSDA). The SSDA corresponds to the well-known mean-field decoupling procedure. For the expectation value in question we obtain

$$\begin{aligned}\langle a^+_{\mathbf{k}-\mathbf{q}'\sigma}\hat{\rho}_{\mathbf{q}}a_{\mathbf{k}-\mathbf{q}-\mathbf{q}'\sigma}\rangle \approx & \sum_{\mathbf{p}\sigma'}\delta_{\mathbf{q},0}\langle a^+_{\mathbf{k}-\mathbf{q}'\sigma}a_{\mathbf{k}-\mathbf{q}-\mathbf{q}'\sigma}\rangle \\ & \times\langle a^+_{\mathbf{p}\sigma'}a_{\mathbf{p}+\mathbf{q}\sigma'}\rangle \\ & -\sum_{\mathbf{p}\sigma'}\delta_{\mathbf{p},\mathbf{k}-\mathbf{q}-\mathbf{q}'}\delta_{\sigma,\sigma'}\langle a^+_{\mathbf{k}-\mathbf{q}'\sigma}a_{\mathbf{p}+\mathbf{q}\sigma'}\rangle \\ & \times\langle a^+_{\mathbf{p}\sigma'}a_{\mathbf{k}-\mathbf{q}-\mathbf{q}'\sigma}\rangle. \end{aligned}\tag{46}$$

Dropping again the $\mathbf{q}=0$ term we obtain for the second term in Eq. (27),

$$\begin{aligned} & -\frac{2}{\Omega^2}\sum_{\mathbf{q}\mathbf{q}'}v(\mathbf{q})v(\mathbf{q}')\langle a^+_{\mathbf{k}-\mathbf{q}'\sigma}\hat{\rho}_{\mathbf{q}}a_{\mathbf{k}-\mathbf{q}-\mathbf{q}'\sigma}\rangle \\ & \approx \frac{2}{\Omega^2}\sum_{\mathbf{q}\mathbf{q}'}v(\mathbf{q})v(\mathbf{q}')n_{\mathbf{k}-\mathbf{q}'\sigma}n_{\mathbf{k}-\mathbf{q}-\mathbf{q}'\sigma} \end{aligned}\tag{47}$$

and arrive at the following expression for the nonlocal term within the SSDA,

$$\begin{aligned}\Sigma^{(1)}_{{\rm nl},\mathbf{k}\sigma} = & -\frac{1}{\Omega^2}\sum_{\mathbf{q}\mathbf{q}'}v(\mathbf{q})v(\mathbf{q}')n_{\mathbf{k}-\mathbf{q}-\mathbf{q}'\sigma}(1-2n_{\mathbf{k}-\mathbf{q}\sigma}) \\ & -(\Sigma^{(0)}_{\mathbf{k}\sigma})^2. \end{aligned}\tag{48}$$

This term corresponds to the high-energy limit of diagram (d) in Fig. 1, which exhibits crossed interaction lines and goes substantially beyond the GW approximation [diagram (c) of Fig. 1].

Equation (48) can be rewritten as

$$\Sigma^{(1)}_{{\rm nl},\mathbf{k}} = -\frac{2\alpha r_s}{\pi k}\int_0^\infty dq q\Sigma^{(0)}_q(1-2n_{\mathbf{q}})\ln\left|\frac{k-q}{k+q}\right| - (\Sigma^{(0)}_k)^2. \tag{49}$$

For the sake of internal consistency, the noninteracting momentum distribution of Eq. (38) should be used in Eq. (49).[14] However, to gain some understanding of the influence of correlation we also calculated the SSDA nonlocal term using the QMC momentum distribution. Within this approach the correlation reduces the first-order term at small k and smooths it around $k=1$. This is only a preliminary result which needs to be tested by performing the full QMC calculation of the four-operator expectation value.

In Fig. 7 we show $\Sigma^{(1)}_{\mathbf{k}}$ calculated as a sum of the QMC value of $\Sigma^{(1)}_{\rm loc}$ and the SSDA result for $\Sigma^{(1)}_{{\rm nl},\mathbf{k}}$, using the QMC and the HF momentum distributions. The full term $\Sigma^{(1)}_{\mathbf{k}}$ is reduced compared with its local contribution (dot-dashed line in Fig. 7).

Diagram (d) in Fig. 1 shows the first vertex correction in a $GW\Gamma$ scheme for the self-energy of Eq. (31).[1] Due to the simplified form of the vertex function, any local-field ap-

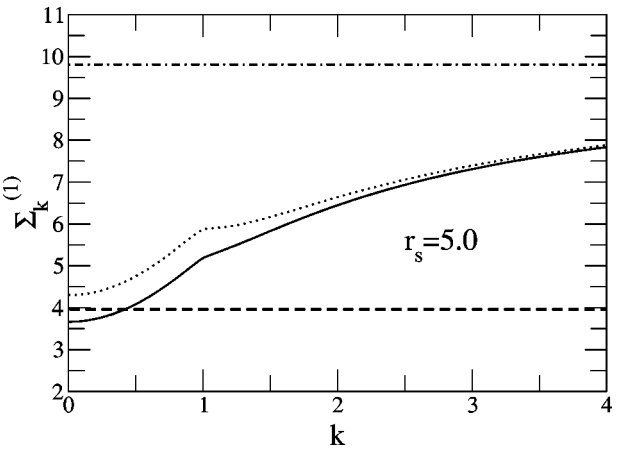

FIG. 7. The first-order term $\Sigma_{\mathbf{k}}^{(1)}$ calculated within the SSDA for $r_s=5.0$ as $\Sigma_{\mathrm{loc}}^{(1)}+\Sigma_{\mathrm{nl},\mathbf{k}}^{(1)}$ using the OB-QMC momentum distribution (solid line) and the HF momentum distribution (dotted line). The dashed line indicates the local (k-independent) correction within VS. As a reference we have also plotted the QMC value of $\Sigma_{\mathrm{loc}}^{(1)}$ (dot-dashed line).

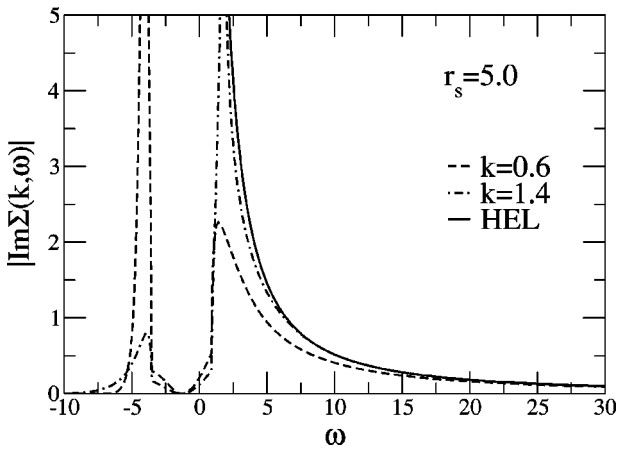

FIG. 8. The imaginary part of the G_0W_0 self-energy at $r_s=5.0$ for two different values of k. In addition we plot the leading term of $|\mathrm{Im}\Sigma(\mathbf{k},\omega)|$ in the high-energy limit (HEL), given by Eq. (51).

proximation along the lines discussed in Sec. IV leads to a local (i.e., k-independent) correction as $\omega\to\infty$. The VS value (dashed line in Fig. 7) comes close to the $k=0$ result of both the QMC-SSDA and the HF-SSDA dispersions, but deviates increasingly at larger values of k. This result shows that the inclusion of nonlocal effects into the vertex function is important.

D. Higher-order terms

After calculating the zeroth- and first-order terms of the self-energy expansion for large frequencies of Eq. (12) we can directly obtain the first and second spectral moments via Eqs. (13) and (14). However, the question remains whether the higher moments are finite, i.e., we have to determine the index n_1 of the last finite moment in the expansions Eqs. (11) and (12).

Instead of using the commutator expression of Eq. (16) we can check the moments $M_{\mathbf{k}\sigma}^{(n)}$ by a direct evaluation of the defining integral of Eq. (9) using the spectral function of Eq. (8). If the imaginary part of the self-energy is zero outside a fixed frequency range, the integral is finite for any power n, and all moments are finite. Otherwise, the convergence of the integral is determined by the high-frequency limit of the integrand, i.e., by the behavior of $\omega^{n-2}|\mathrm{Im}\Sigma(\mathbf{k},\omega)|$ at $\omega\to\pm\infty$. When calculating the imaginary part of the G_0W_0 self-energy in the large-frequency limit, an intermediate step is

$$\mathrm{Im}\Sigma(\mathbf{k}=0,\omega)\sim\sum_{\mathbf{q}} v(\mathbf{q})\mathrm{Im}\epsilon^{-1}[\mathbf{q},\omega-\epsilon_0(\mathbf{q})]. \quad (50)$$

The leading contribution comes from the positive dispersion branch in $\mathrm{Im}\epsilon^{-1}$ and restricts the summation in Eq. (50) via $\omega\approx 2\epsilon_0(\mathbf{q})$ to large values of q. Therefore, the inverse dielectric function can be replaced by the dielectric function itself, $\mathrm{Im}\epsilon^{-1}\to-\mathrm{Im}\epsilon$. With the RPA expression, the integral can be evaluated analytically, which gives the leading term

$$\mathrm{Im}\Sigma(\mathbf{k},\omega)\sim-\frac{16\sqrt{2}}{3\pi}\frac{(\alpha r_s)^2}{\omega^{3/2}}=-\frac{C}{\omega^{3/2}},\quad \omega\to+\infty. \quad (51)$$

Consequently, the integrand for the nth moment behaves as $\omega^{n-2-3/2}$ at large positive frequencies, and the last finite moment is obtained for $n=2$. In Fig. 8 we display the imaginary part of the G_0W_0 self-energy and its limiting behavior given by Eq. (51).

We have analyzed the other diagrams to second order in the bare Coulomb potential and found that only the vertex diagram in Fig. 1(d) contributes to the $1/\omega^{3/2}$ term in the high-energy limit as

$$\mathrm{Im}\Sigma^{\Gamma}(\mathbf{k},\omega)\sim+\frac{1}{2}\frac{C}{\omega^{3/2}},\quad \omega\to+\infty, \quad (52)$$

where C is defined by Eq. (51). From general considerations we expect that the contributions of all higher-order diagrams in the high-energy expansion of $\mathrm{Im}\Sigma$ decay faster than $1/\omega^{3/2}$. Therefore we conclude quite generally that in the HEG, $n_1=2$, and therefore the spectral moments $M_{\mathbf{k}}^{(0)}=1$, $M_{\mathbf{k}}^{(1)}$ and $M_{\mathbf{k}}^{(2)}$ are the only finite ones. This surprising result can be understood if one notes (1) that the electron dispersion $\epsilon_0(\mathbf{q})$ is unlimited at positive energies and (2) that the basic interaction potential $v(\mathbf{q})$ has a power-law dependence at large momentum transfer $\mathbf{q}$ (here q^{-2}).

We have also analyzed the high-energy limit of the imaginary part of the self-energy in the local-field approximation, defined by Eqs. (31), (32), and (34), and find that

$$\mathrm{Im}\Sigma^{f}(\mathbf{k},\omega)\sim-[1-f(q\to\infty)]\frac{C}{\omega^{3/2}},\quad \omega\to+\infty, \quad (53)$$

where C is defined by Eq. (51). For the Hubbard local-field factor we have $f(q\to\infty)=1/2$, thus reproducing exactly the sum of the terms defined by Eqs. (51) and (52) in the high-energy limit of $\mathrm{Im}\Sigma^f(\mathbf{k},\omega)$.

The general relation between the high-frequency limit of $\mathrm{Im}\Sigma$ and the spectral moments works in both directions. If the commutation relation of Eq. (16) produces finite results up to order n_1, the imaginary part of the exact self-energy decays faster than $\omega^{-(n_1-1)}$.

VI. CONCLUSION AND OUTLOOK

We have derived analytic expressions for the lowest three moments of the spectral function of the one-particle Green's function of the three-dimensional HEG. These moments are related to the zeroth and first coefficients in the expansion of the self-energy in inverse powers of the frequency.

The zeroth-order term in the high-energy expansion was calculated using the HF, G_0W_0, and QMC momentum distributions. We established that the use of different parametrizations of the QMC data does not change the numerical results for the zeroth-order term significantly. The G_0W_0 and QMC data gives first moments which are significantly larger than the HF values below the Fermi edge and very close to them above the Fermi edge. The G_0W_0 result does not differ significantly from the QMC data.

The first-order term in the high-energy expansion can be written as the sum of a local and a nonlocal term. For the HEG, we have shown that the local term can be rewritten in terms of the static structure factor. We have calculated the local term within various approximations, including a parametrization of the QMC data for the structure factor.

We have performed an approximate calculation of the nonlocal term in the SSDA, which indicates that it is large and has a strong k dependence. The local part is positive, but the nonlocal part is negative and therefore leads to a substantial reduction in the size of the first-order term and the corresponding second moment of the spectral function. We have identified the nonlocal term in the SSDA with the high-energy limit of the first vertex correction beyond GW. A QMC calculation of the nonlocal term would be very useful, and this will be addressed in a forthcoming paper. We have shown for different approximations that higher moments are divergent and concluded that this is a general property of the HEG.

Our results provide additional benchmarks for self-energy theories of the HEG and might help in resolving the current debate concerning the valence bandwidth of alkali metals.

ACKNOWLEDGMENTS

M.V. and R.J.N. acknowledge the Engineering and Physical Sciences Research Council (UK) for funding, and M.V. acknowledges the Gottlieb Daimler- und Karl Benz-Stiftung (Ladenburg, Germany) for their financial support.

APPENDIX A: DERIVATION OF THE FIRST MOMENT

For the derivation of the moments we use the following commutation relations which are derived from the anticommutation relations of the fermionic operators and the expression for the density operator given in Eq. (2),

$$[a_{\mathbf{k}\sigma},\hat{\rho}_{\mathbf{q}}]_-=a_{\mathbf{k}+\mathbf{q}\sigma},\quad [a^+_{\mathbf{k}\sigma},\hat{\rho}_{\mathbf{q}}]_-=-a^+_{\mathbf{k}-\mathbf{q}\sigma}. \tag{A1}$$

According to Eq. (16) the first moment is

$$M^{(1)}_{\mathbf{k}\sigma}=\langle[[a_{\mathbf{k}\sigma},\hat{H}]_-,a^+_{\mathbf{k}\sigma}]_+\rangle. \tag{A2}$$

Decomposing the Hamiltonian of Eq. (1) into the free and the interacting part, $\hat{H}=\hat{H}_1+\hat{H}_2$, we calculate

$$[[a_{\mathbf{k}\sigma},\hat{H}_1]_-,a^+_{\mathbf{k}\sigma}]_+=\epsilon_0(\mathbf{k}). \tag{A3}$$

Using

$$[a_{\mathbf{k}\sigma},\hat{\rho}_{\mathbf{q}}\hat{\rho}_{-\mathbf{q}}]_-=2\hat{\rho}_{\mathbf{q}}a_{\mathbf{k}-\mathbf{q}\sigma}+a_{\mathbf{k}\sigma},\quad [a_{\mathbf{k}\sigma},\hat{N}]_-=a_{\mathbf{k}\sigma}, \tag{A4}$$

we obtain

$$[a_{\mathbf{k}\sigma},\hat{H}_2]_-=\frac{1}{2\Omega}\sum_{\mathbf{q}}v(\mathbf{q})\hat{\rho}_{\mathbf{q}}a_{\mathbf{k}-\mathbf{q}\sigma}. \tag{A5}$$

Therefore

$$\begin{aligned}[[a_{\mathbf{k}\sigma},\hat{H}_2]_-,a^+_{\mathbf{k}\sigma}]_+&=\frac{1}{\Omega}\sum_{\mathbf{q}}v(\mathbf{q})[\hat{\rho}_{\mathbf{q}}a_{\mathbf{k}-\mathbf{q}\sigma},a^+_{\mathbf{k}\sigma}]_+\\&=-\frac{1}{\Omega}\sum_{\mathbf{q}}v(\mathbf{q})a^+_{\mathbf{k}-\mathbf{q}\sigma}a_{\mathbf{k}-\mathbf{q}\sigma}.\end{aligned} \tag{A6}$$

Adding Eqs. (A3) and (A6) and taking the expectation value we arrive at Eq. (18).

APPENDIX B: DERIVATION OF THE SECOND MOMENT

According to Eq. (16) the second moment is given by

$$\begin{aligned}M^{(2)}_{\mathbf{k}\sigma}&=\langle[[[a_{\mathbf{k}\sigma},\hat{H}]_-,\hat{H}]_-,a^+_{\mathbf{k}\sigma}]_+\rangle\\&=\langle[[[a_{\mathbf{k}\sigma},\hat{H}_1]_-,\hat{H}_1]_-,a^+_{\mathbf{k}\sigma}]_+\rangle\\&\quad+2\langle[[[a_{\mathbf{k}\sigma},\hat{H}_1]_-,\hat{H}_2]_-,a^+_{\mathbf{k}\sigma}]_+\rangle\\&\quad+\langle[[[a_{\mathbf{k}\sigma},\hat{H}_2]_-,\hat{H}_2]_-,a^+_{\mathbf{k}\sigma}]_+\rangle.\end{aligned} \tag{B1}$$

The first two expectation values in Eq. (B1) are easily evaluated as

$$\langle[[[a_{\mathbf{k}\sigma},\hat{H}_1]_-,\hat{H}_1]_-,a^+_{\mathbf{k}\sigma}]_+\rangle=[\epsilon_0(\mathbf{k})]^2, \tag{B2}$$

$$\langle[[[a_{\mathbf{k}\sigma},\hat{H}_1]_-,\hat{H}_2]_-,a^+_{\mathbf{k}\sigma}]_+\rangle=\epsilon_0(\mathbf{k})\Sigma^{(0)}_{\mathbf{k}\sigma}. \tag{B3}$$

For the third term in Eq. (B1) we require the following commutator,

$$[[a_{\mathbf{k}\sigma},\hat{H}_2]_-,\hat{H}_2]_-$$
$$=\frac{1}{2\Omega^2}\sum_{\mathbf{q}} v(\mathbf{q})\sum_{\mathbf{q}'} v(\mathbf{q}')[\hat{\rho}_{\mathbf{q}}a_{\mathbf{k}-\mathbf{q}\sigma},\hat{\rho}_{\mathbf{q}'}\hat{\rho}_{-\mathbf{q}'}]_-$$
$$-\frac{1}{2\Omega^2}\sum_{\mathbf{q}} v(\mathbf{q})\sum_{\mathbf{q}'} v(\mathbf{q}')[\hat{\rho}_{\mathbf{q}}a_{\mathbf{k}-\mathbf{q}\sigma},\hat{N}]_-.$$

Using

$$[\hat{\rho}_{\mathbf{q}}a_{\mathbf{k}-\mathbf{q}\sigma},\hat{\rho}_{\mathbf{q}'}\hat{\rho}_{-\mathbf{q}'}]_-=\hat{\rho}_{\mathbf{q}}a_{\mathbf{k}-\mathbf{q}\sigma}+2\hat{\rho}_{\mathbf{q}}\hat{\rho}_{\mathbf{q}'}a_{\mathbf{k}-\mathbf{q}-\mathbf{q}'\sigma},$$

and

$$[\hat{\rho}_{\mathbf{q}}a_{\mathbf{k}-\mathbf{q}\sigma},\hat{N}]_-=\hat{\rho}_{\mathbf{q}}a_{\mathbf{k}-\mathbf{q}\sigma}, \tag{B4}$$

one arrives at the following expression,

$$[[a_{\mathbf{k}\sigma},\hat{H}_2]_-,\hat{H}_2]_-=\frac{1}{\Omega^2}\sum_{\mathbf{q}} v(\mathbf{q})\sum_{\mathbf{q}'} v(\mathbf{q}')\hat{\rho}_{\mathbf{q}}\hat{\rho}_{\mathbf{q}'}a_{\mathbf{k}-\mathbf{q}-\mathbf{q}'\sigma}.$$

With Eq. (A1) and

$$[\hat{\rho}_{\mathbf{q}},a^+_{\mathbf{k}-\mathbf{q}'\sigma}]_-=a^+_{\mathbf{k}-\mathbf{q}-\mathbf{q}'\sigma}, \tag{B5}$$

we finally obtain

$$[[[a_{\mathbf{k}\sigma},\hat{H}_2]_-,\hat{H}_2]_-,a^+_{\mathbf{k}\sigma}]_+$$
$$=\frac{1}{\Omega^2}\sum_{\mathbf{q}} v(\mathbf{q})\sum_{\mathbf{q}'} v(\mathbf{q}')[\hat{\rho}_{\mathbf{q}}\hat{\rho}_{\mathbf{q}'}a_{\mathbf{k}-\mathbf{q}-\mathbf{q}'\sigma},a^+_{\mathbf{k}\sigma}]_+$$
$$=\frac{1}{\Omega}\sum_{\mathbf{q}} v^2(\mathbf{q})\hat{\rho}_{\mathbf{q}}\hat{\rho}_{-\mathbf{q}}-\frac{1}{\Omega^2}\sum_{\mathbf{q}} v(\mathbf{q})$$
$$\times\sum_{\mathbf{q}'} v(\mathbf{q}')a^+_{\mathbf{k}-\mathbf{q}-\mathbf{q}'\sigma}a_{\mathbf{k}-\mathbf{q}-\mathbf{q}'\sigma}$$
$$-\frac{2}{\Omega^2}\sum_{\mathbf{q}} v(\mathbf{q})\sum_{\mathbf{q}'} v(\mathbf{q}')a^+_{\mathbf{k}-\mathbf{q}'\sigma}\hat{\rho}_{\mathbf{q}}a_{\mathbf{k}-\mathbf{q}-\mathbf{q}'\sigma}. \tag{B6}$$

With the definitions of Eqs. (B2) and (B3) we arrive at Eq. (22).

[1] G.D. Mahan, *Many-Particle Physics* (Plenum, New York, 1981).
[2] H. Yasuhara, S. Yoshinaga, and M. Higuchi, Phys. Rev. Lett. **83**, 3250 (1999).
[3] H. Yasuhara, S. Yoshinaga, and M. Higuchi, J. Phys. Soc. Jpn. **68**, 3473 (1999).
[4] Y. Takada, Phys. Rev. Lett. **87**, 226402 (2001).
[5] E. Jensen and E.W. Plummer, Phys. Rev. Lett. **55**, 1912 (1985).
[6] I.W. Lyo and E.W. Plummer, Phys. Rev. Lett. **60**, 1558 (1988).
[7] W.M.C. Foulkes, L. Mitas, R.J. Needs, and G. Rajagopal, Rev. Mod. Phys. **73**, 33 (2001).
[8] U. von Barth and B. Holm, Phys. Rev. B **54**, 8411 (1996).
[9] B. Holm and U. von Barth, Phys. Rev. B **57**, 2108 (1997).
[10] M. Hindgren and C.O. Almbladh, Phys. Rev. B **56**, 12 832 (1997).
[11] A. Schindlmayr, T.J. Pollehn, and R.W. Godby, Phys. Rev. B **58**, 12 684 (1998).
[12] B. Holm and F. Aryasetiawan, Phys. Rev. B **62**, 4858 (2000).
[13] P. Garcia-Gonzalez and R.W. Godby, Phys. Rev. B **63**, 075112 (2001).
[14] B. Farid, Philos. Mag. B **82**, 1413 (2002).
[15] W. Nolting, *Grundkurs Theoretische Physik* (Springer, Berlin, 2002), Vol. 7, p. 129.
[16] L. Hedin, Phys. Rev. **139**, A796 (1965).
[17] L. Hedin and S. Lundqvist, *Solid State Physics* (Academic, New York, 1969), Vol. 23, p. 1.
[18] W. Ku, A.G. Eguiluz, and E.W. Plummer, Phys. Rev. Lett. **85**, 2410 (2000); H. Yasuhara, S. Yoshinaga, and M. Higuchi, *ibid.* **85**, 2411 (2000).
[19] B. Holm and F. Aryasetiawan, Phys. Rev. B **56**, 12 825 (1997).
[20] G.D. Mahan and B.E. Sernelius, Phys. Rev. Lett. **62**, 2718 (1989).
[21] J. Hubbard, Proc. R. Soc. London, Ser. A **243**, 336 (1957).
[22] K.S. Singwi, M.P. Tosi, R.H. Land, and A. Sjölander, Phys. Rev. **176**, 589 (1968).
[23] P. Vashishta and K.S. Singwi, Phys. Rev. B **6**, 875 (1972).
[24] J.E. Northrup, M.S. Hybertsen, and S.G. Louie, Phys. Rev. Lett. **59**, 819 (1987).
[25] C. Petrillo and F. Sacchetti, Phys. Rev. B **38**, 3834 (1988).
[26] B.I. Lundqvist, Phys. Kondens. Mater. **7**, 117 (1968).
[27] D.M. Ceperley and B.J. Alder, Phys. Rev. Lett. **45**, 566 (1980).
[28] G. Ortiz, M. Harris, and P. Ballone, Phys. Rev. Lett. **82**, 5317 (1999).
[29] G. Ortiz and P. Ballone, Phys. Rev. B **50**, 1391 (1994); **56**, 9970(E) (1997).
[30] G. Senatore, S. Moroni, and D. Ceperley, in *Physics of Strongly Coupled Plasmas*, edited by W.D. Kraeft (World Scientific, Singapore, 1995).
[31] P. Gori-Giorgi and P. Ziesche, Phys. Rev. B **66**, 235116 (2002).
[32] P. Gori-Giorgi, F. Sacchetti, and G.B. Bachelet, Phys. Rev. B **61**, 7353 (2000); **66**, 159901(E) (2002).
[33] Subroutines for evaluating the fitting formulas for the momentum distribution of Gori-Giorgi and Ziesche (Ref. 31) and the structure factor of Gori-Giorgi, Sacchetti, and Bachelet (Ref. 32) can be found at http://axtnt2.phys.uniroma1.it/PGG/elegas.html
[34] In his paper (Ref. 14), Farid claims this term can be made convergent by a regularization of this integral. This regularization is, in our view, inappropriate.